ISSN 1590-8844
International Journal of Mechanics and Control, Vol. 17, No. 01, 2016

APPLICATIONS OF ADVANCED SIGNAL PROCESSING ANALYSIS

Vincenzo Niola * Giuseppe Quaremba **

* Università di Napoli Fedrico II, Dipartimento di Ingegneria Industriale

** Dipartimento di Scienze Biomediche Avanzate

ABSTRACT

Nowadays, in the industrial field, the predictive maintenance is an important methodology employed for reducing risks of machine stops. Machines are continuously monitored in order to maximize the performance, both in terms of quality and productivity. In this paper it is pointed out an advanced methodology of signal processing which allows to evaluate in advance which kind of fault can happen on a machinery. Several applications are presented in order to show the main features of the method.

Keywords: Signal processing, Industrial Diagnostic, Wavelet Transform.

1 INTRODUCTION

The Wavelet Transform (WT) [Daubechies I., Ten Lectures on Wavelets, SIAM, 1992] represents a time-scale analysis of the smoothness of a signal or, more in general, of a time series or a curve profile. The Wavelet analysis, unlike the FFT, is very useful when one analyzes and decompose signal with a not constant frequency. Qualitatively, the difference between the usual sine wave and a wavelet can be described from the localization property: the sine wave is localized in frequency domain, but not in time domain, while a wavelet is localized both in the frequency and time domain. Furthermore, the duration of its maximum oscillation is relatively small. One can regard a wavelet is a shape of wave of limited duration and zero moments of a given order. The choice of a wavelet and of signal decomposition level depends on the shape of signals and on the experience of the analyst. For its versatility, the wavelet analysis is diffused in many fields, such as Acoustics, Electrodynamics [Kaiser G., A Friendly Guide to Wavelets, Birkhäuser, 1999], Finance [Härdle W. et al. Lecture Notes in Statistics - Wavelets, Approximation, and Statistical Applications, Springer, 1998] Medicine and Statistics [Antoniadis A., Oppenheim G., Lecture notes in Statistics - Wavelets and Statistics, Springer, 1995]. In particular, the wavelets used in this paper are those proposed by Daubechies (1992).

Contact author: Vincenzo Niola

E-mail: vincenzo.niola@unina.it

She constructed a series of mather wavelets (indexed by N and denoted by db$N$) with each mother in the series having regularity proportional to N. Each Daubechies' wavelet is compactly supported in the time domain.
Typically wavelets of class m, are specifically constructed so that some properties are verified (Meyer Y., Wavelets and operators, Cambridge University Press, 2004), [1-4].
A mother wavelet ψ is a function of zero h-th moment:

$$\int_{-\infty}^{+\infty} x^h \psi(x)dx = 0\,, \quad h \in \mathbf{N}. \tag{1}$$

From this definition, it follows that, if ψ is a wavelet whose all moments are zero, also the function ψ_{ik} is a wavelet, where

$$\psi_{jk}(x) = 2^{j/2}\psi(2^j x - k)\,. \tag{2}$$

In fact, we have

$$\int_{-\infty}^{+\infty} 2^{j/2} x^h \psi(2^j x - k)dx =$$

$$= 2^{j/2}\int_{-\infty}^{+\infty} \frac{1}{2^j}\left(\frac{y+k}{2^j}\right)^h \psi(y)dy =$$

$$= \frac{2^{j/2}}{2^{j(h+1)}}\int_{-\infty}^{+\infty} (y+k)^h \psi(y)dy =$$

$$= \frac{2^{j/2}}{2^{j(h+1)}}\sum_{m=0}^{h}\binom{h}{m} k^{h-m}\int_{-\infty}^{+\infty} y^m \psi(y)dy = 0. \tag{3}$$

Moreover, consider a wavelet ψ and a function φ such that $\{\{\varphi_{j_0k}\}, \{\psi_{jk}\}, k \in \mathbf{Z}, j = 0, 1, 2,\ldots\}$ is a complete orthonormal system. By Parseval theorem, for every s $\in$ $L_2(\mathbf{R})$, it follows that

$$s(t) = \sum_k a_{j_0k}\varphi_{j_0k}(t) + \sum_{j=j_0}^{j_1}\sum_k d_{jk}\psi_{jk}(t) . \tag{4}$$

The decomposition of a signal $s(t)$ by wavelet is represented by the following detail function coefficients:

$$d_{jk} = \int_{-\infty}^{+\infty} s(\tau)\cdot\frac{1}{\sqrt{2^j}}\psi\left(\frac{\tau-k}{2^j}\right)d\tau \tag{5}$$

and by the approximating scaling coefficients

$$a_{j_0k} = \int_{-\infty}^{+\infty} s(\tau)\cdot\psi(\tau-k)d\tau . \tag{6}$$

Note that d_{jk} can be regarded, for any j, as a function of k. Consequently, it is constant if the signal $s(t)$ is a smooth function, having considered that a wavelet has zero moments. To show the above mentioned property, it is sufficient to expand the signal in Taylor's series.

2 APPLICATIONS

In this paragraph some applications of the theory and of the technique, summarized above, are presented in order to both show the technique and validate it

2.1 EXHAUST GAS RECIRCULATION EVALUATION

The first application is the reduction of emissions of NOx through the technique called Exhaust Gas Recirculation (EGR). The policy of reducing emissions in the energy sector is one of the scientific community's main research topics. There have been significant developments in automotive and business fields, particularly in diesel engines. Nowadays, the method, which is widely used in reducing emissions of a Diesel engine, is the dilution factor called EGR through which it is possible to lower NOx levels. The adoption of sophisticated signal processing method such as the one presented in the following, allows easier control of complex systems such as diesel systems Homogeneous Charge Compression Ignition (HCCI), [5–10]. The proposed method of signal processing is the verification of the following basic idea: an engine fueled with a greater amount of inert (*i.e.*, gas recirculation) should exhibit, if it is compared to a standard power supply, a more regular operating condition. The experimental set-up is presented in Fig. 1; the engine test bench has been equipped to test a 1910 cm^3 Common Rail Diesel engine. The main two methodological conditions applied are as follows: i- stationary running of the engine during all the test-run; ii- working points set at 2000rpm and 2bar regarding the mean effective pressure (MEP). The engine is set on standard running conditions (*i.e.*, amount of recirculated gas equal to that normally used by the standard mapping of the motor). These data are used to construct the so-called "reference signal" (baseline).

Subsequent acquisitions are obtained by varying the set-up of the solenoid regulating the EGR in order to gradually increase the amount of exhaust gas in the combustion chamber (performed by means of 5 very small steps, *i.e.*, with the EGR ratio starting from 2.0 and increasing of 1%, until a final value of 2.2) causes a less abrupt combustion with lower local peak of temperature and consequently less formation of nitrogen oxides (NOx).

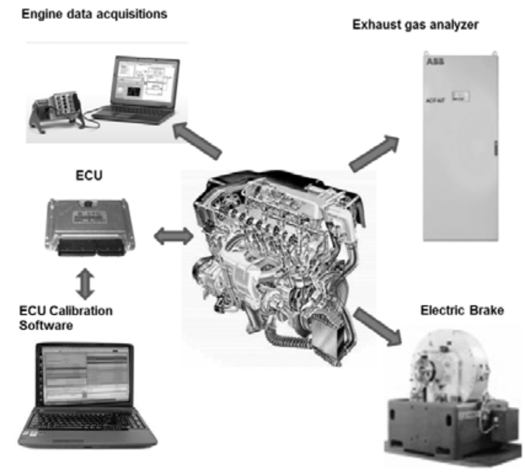

Figure 1 Engine test equipment.

Recall that the purpose of the test was to quantify the "degree of regularity" of the engine for the several set-ups of the EGR (called EGR1, EGR2, etc.) by processing only the accelerometer signals acquired during the test-run.
The measurements are referred to the morphodynamical vibration shown by the engine when it is powered with a gradual increase of the percentage of inert. To obtain this weak information from each cluster (baseline, EGR1, etc.) the accelerometer signals are "synchronized" with the tachometer signal acquired during the running-test. In order to evaluate such a phenomenon, a signal named "surrogate" has been reconstructed for each cluster. It is representative of an averaged class of frequencies and amplitudes) obtained during the test-run (baseline and EGRs). For the construction of a "surrogate" see [10].
Fig. 2 shows the comparison between the surrogates extracted from each cluster. It is quite clear that the higher the percentage of EGR, the greater its phase shift and amplitude. In particular, the change of the surrogate signals can be observed in terms of amplitude and frequency, depending on the cluster from which they were extracted.
Now the problem is to discriminate among groups in order to distinguish them. For example, if a certain "maneuver" can lead to an important and significant response of the engine, variables play a crucial role in attaining the target: to discriminate among the groups. Therefore, to achieve this goal one or more linear combinations of variables must be built in order to discriminate the clusters in the following form:

$$D_i = w_{i1}Z_1 + w_{i2}Z_2 + \ldots\ldots + w_{ip}Z_p \tag{7}$$

ISSN 1590-8844
International Journal of Mechanics and Control, Vol. 17, No. 01, 2016

where D_i is the score of the i^{th} discriminant function, w are the weights given by each variable, Z are the standardized values of the p variables used in the analysis.

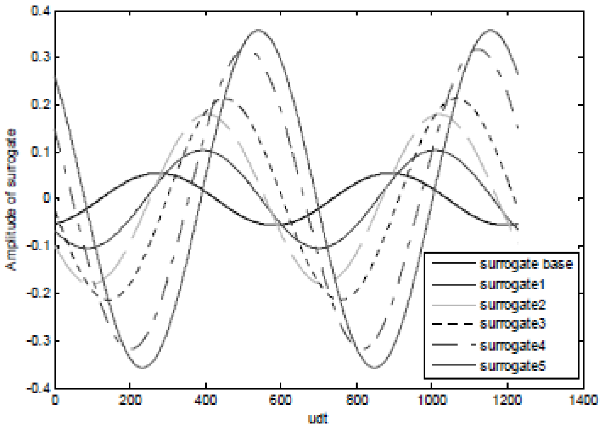

Figure 2 Comparison of 6 surrogates.

Fig. 3 shows how these parameters, defined above, help the classification of the 306 accelerometer signals. Fig. 3shows the presence of 6 well "discriminated" clusters. In particular, we observe EGR1, generated by the minimum change of the EGR ratio, (in terms of percentage from EGR ratio 2.0 of baseline to 2.02 of EGR1). The correlation coefficient (Fig. 4) shows a rather rapid increase from the baseline condition up to the set-up of EGR1, reaching the maximum under the set-up referred to as EGR4. It is clear the reduction of the correlation at EGR5 set-up, beyond which any further supply of inert gas, may affect the smooth vibrational running of the engine. The correlation coefficient confirms that an engine powered with exhaust gas recirculation produces a vibrational signature very similar to its surrogate and therefore very repetitive (about +40%). Conversely, the engine not powered by exhaust gas has a more irregular trend (about -25 %).

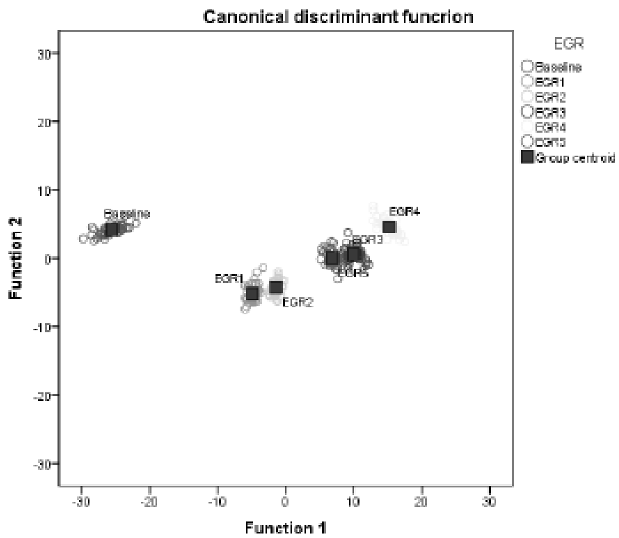

Figure 3 Classification map (306 records).

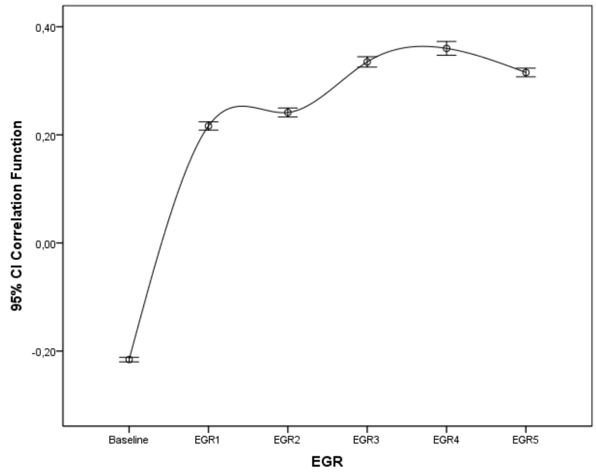

Figure 4 Correlation coefficient (306 records).

It must be remembered that correlation measure how variables are related. Before calculating a correlation coefficient, data were screened for outliers (which can cause misleading results) and evidence of a linear relationship. Pearson's correlation coefficient is a measure of linear association. Two variables can be perfectly related, but if the relationship is not linear, Pearson's correlation coefficient is not an appropriate statistic for measuring their association. However, the Pearson correlation coefficient works best when the variables are approximately normally distributed and have no outliers.

The correlation coefficient range is -1÷+1, the greater is the coefficient the greater is the relationship between the variables viz between EGR and vibrations.

Thanks to its response and sensitivity, the proposed method could be used to optimize, for example, the curve of EGR for each engine family, using the response of the mechanical system in terms of vibration.

2.2 ANALYSIS OF THE PERFORMANCE OF AN INTERNAL COMBUSTION ENGINE

The second application is a methodology for identifying and analysing the performance of an Internal Combustion (I.C.) engine and, at the same time, for the reconstruction of the morphodynamical vibration. In particular, the purpose of the method, showed in this paper, is to assess the performance of an I.C. engine trough the degree of vibrational regularity of each cylinder and, at the same time, to build a diagram characterizing the functional performance, averaged over a significant number of revolutions (namely 60 and 120). The response is processed by means of the wavelet multiresolution analysis [11].

In particular, in the following we introduce the method for the determination of the morpho-dynamical vibration performed during the combustion stage where the highest in-cylinder pressure is reached (IPv) as well as the instantaneous vibrational mean in-cylinder pressure (MIPv). The vibration monitoring was performed on the I.C. engine of a cargo ship during a commercial navigation.

The acquisition of the accelerometric signals for deriving the vibrational signatures characterizing, in particular, each cylinder, was performed by using the same unidirectional accelerometers placed on each cylinder (Fig. 5).
The synchronization was performed by means a tacho detector was placed on a toothed wheel keyed on the motor shaft. Accelerometric signals were sampled continuously at 20480 samples/s (sampling frequency) for a duration of approximately 5min, for several settings and conditions. In the following we reported the most statistically significant results: at 114 rpm, 75% cargo condition.
The measurements were performed by placing the accelerometers on the following three locations (*i.e.*, levels) of the engine: 1l - Base; 2l - Level of collector lubricating oil recovery; 3l - Level close to the motor head. With reference to the six cylinders, it does not appreciate any significant difference with the usual spectral-shape analysis.

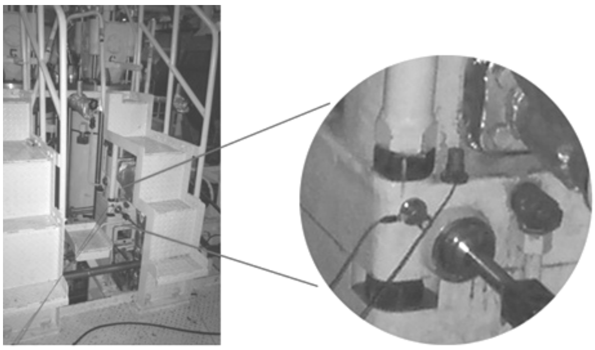

Figure 5 Accelerometer location.

The Figure 6 illustrates the spectral diagram where are highlighted the main frequencies due to several mechanical components. For instance, the 9.5Hz frequency is caused by the propeller while the 11.5Hz frequency is generated by the engine system. The 95Hz frequency is due to the chain drive wheel (50 teeth). The 45.5Hz is the frequency due to the tensioner (wheel of 25 teeth) while the 60Hz is the power generator.

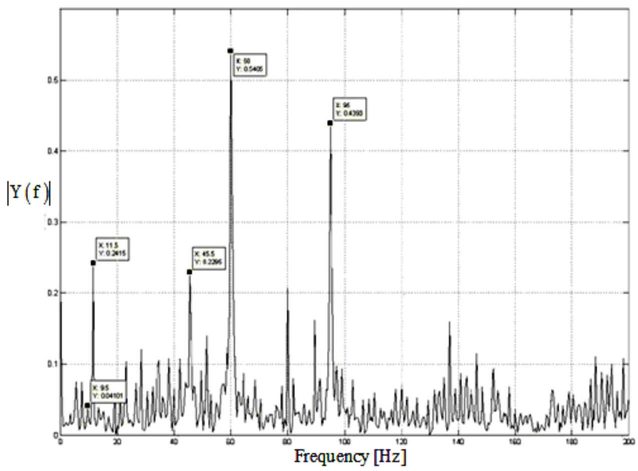

Figure 6 Working spectrum.

As *working spectrum* we mean the frequency spectrum due to typical concentrated masses. The spectrum, in the case of correct operation of the system (*i.e.*, the entire propulsion system chain), provides the basic frequencies of each component and their coupling with the ship system. A very important and critical stage of the monitoring phase was to detect the vibrational signatures as well as the performance exhibited by each cylinder during the evolution of the respective thermodynamic cycle. The Fig. 7 illustrates the importance of employing a method (based on the WT) that allows both the aimed selection of the working frequency and the reconstruction of temporal evolution of the phenomenon spectrally selected. In particular, the speed was 12 rad/s, it was used a single accelerometer placed on the head of the cylinder no. 6, with the z axis parallel to the main direction of the cylinder. The instantaneous vibrational sequence (*i.e.*, the wavelet coefficients), generated by the thermodynamic cycle (corresponding to the self-ignition of the fuel), is shown in Fig. 7.

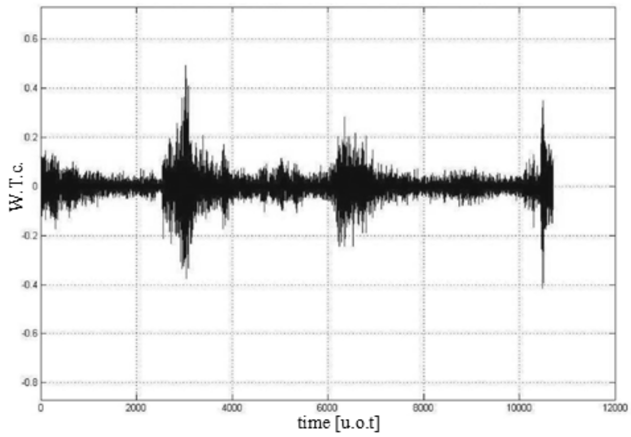

Figure 7 Wavelet coefficients at 12 rad/s.

The Fig. 8 compares the vibrational diagrams geometrically averaged of cylinder no.1, reconstructed with 20 harmonics after 13, 60 and 120 periods; the stability of the shape suggests for a good reliability of the method used for the reconstruction of the *morphodynamical* vibration. We use the word morphodynamical because the extraction of the wavelet coefficients allows the evaluation of both the morphology and the dynamic of the mechanical system vibration. Starting from the accelerometric signal, the method was applied to the other cylinders. Figure 9 shows the comparison of the aforesaid vibrational signatures due to the three cylinders: 1, 3 and 6. We note a significant difference both of the shape and of the area under the cyl no. 6. The method indirectly shows also the performance of the thermodynamic cycles of a crank-slider mechanical system. In particular, it provides important information about the ignition and the combustion phases, within 60° of crank-angle, where it depends the regularity of running and consequently the stress distribution on several mechanical components as well as the chain of cam-shaft, which is, of course, the weakest link of the mechanical arrangement.

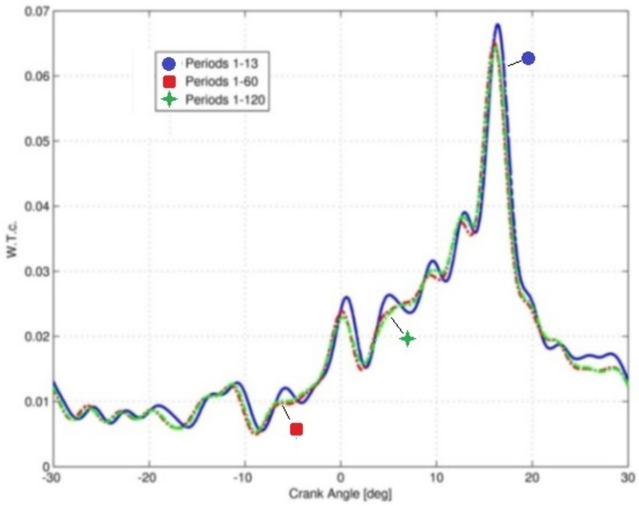

Figure 8 Comparison of MIPv at 13,60 and 120 periods (cylinder no. 1).

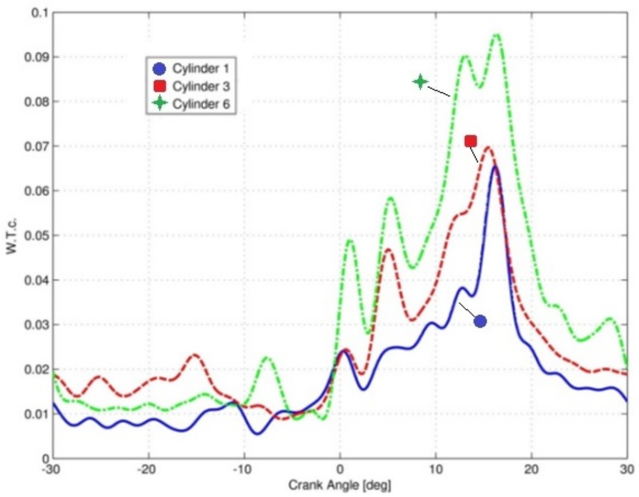

Figure 9 Comparison of MIPv of cylinders no. 1, 3 and 6.

A best performance for the analysis of thermodynamic cycles is achieved by involving also the thermal images detected trough infrared camera integrated with the technique of Wavelet Transform [12].

2.3 GRASPING ANALYSIS OF MECHANICAL HAND

A further application of the proposed technique consists in examining the signals of accelerometers fitted on the phalanxes of a mechanical hand representing a hand prosthesis prototype. This device was designed and built at the laboratory of Robotics of the D.I.I. of the University of Naples “Federico II”, [13-15].

A prototype, instrumented with the accelerometers is shown in Figure 10. In the same figure it is possible to observe the hand while grasping a wooden sphere having 42 mm diameter. By examining the signals while the object is grasped, it is possible to recognize if and how instability of the grasping occurs.

Moreover two different laws of motion were adopted for the only actuator during the grasping. For both the laws of motion the maximum actuator force is 40 N, but this amount is reached in 0.2 seconds in the first case and in 0.4 in the other case. In the following we will indicate with f_1 the first law of motion and with f_2 the second one.

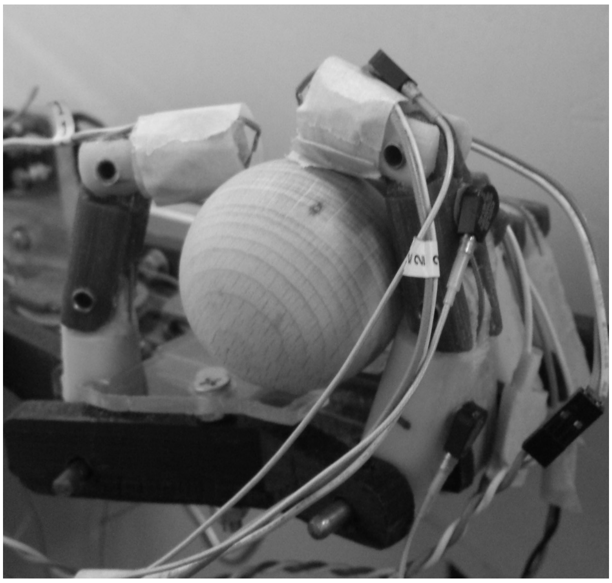

Figure 10 Hand prototype grasping a sphere.

In Figure 11 and 12 the signals by the accelerometers are reported. Figure 11 refers to the f_1 law of motion, while Figure 12 refers to f_2. How it is possible to observe, during the first 0.1 second the phalanxes of the finger approach the object and grasp it. After about 0.1 second, the phalanxes are onto contact with the object surface. During the next 0.4 seconds, the accelerometer signal doesn’t show significant accelerations, thus no significant changes in the grasping occur.

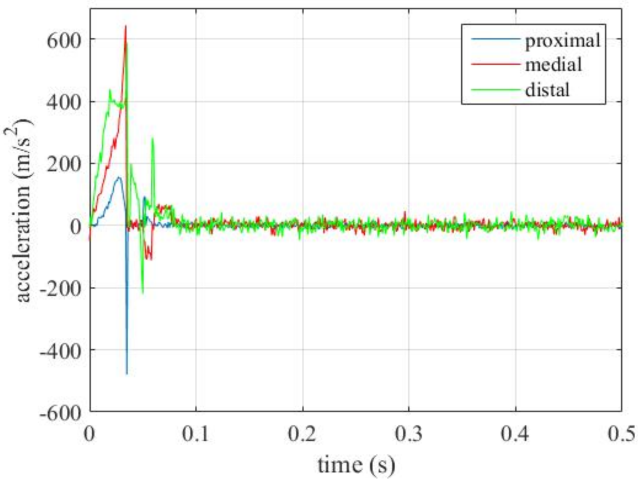

Fig. 11 Accelerometers signals with f_1 closing law of motion.

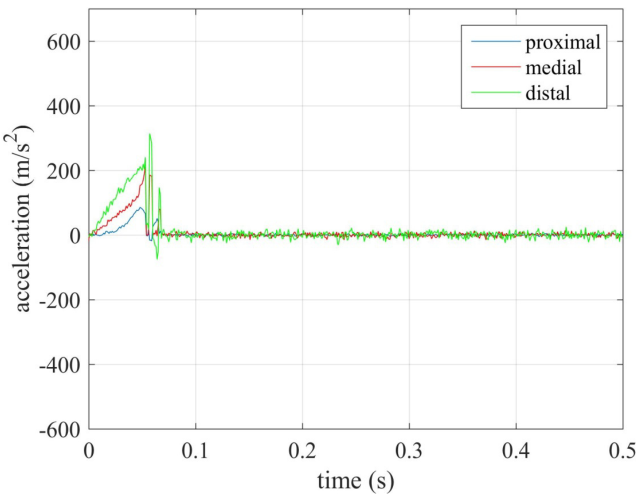

Fig. 12 Accelerometers signals with f_2 closing law of motion.

If Figure 11 and 12 are compared, it is clear that the different actuator laws of motion play a significant role both during the early phase of the grasping and also during the phase of the object holding; in fact the acceleration during the first 0.05 seconds is higher in the case of f_1 law of motion and, moreover, during the holding phase. The above suggests that suitable laws of motion of the actuator could be planned, for example by using the methods already proposed and studied in [16,17] for the motion planning of the links of a robot.

5 CONCLUSIONS

A signal processing analysis method was presented with some application examples. The main advantages of the proposed method can be summarized as follows:

1. It does not require expensive equipment;
2. it is very flexible;
3. it is fast;
4. it does not require maintenance.

Moreover, the proposed method is non-invasive, it is reliable and easy to implement. It could be performed a real-time system monitoring. The results, referred to the pressure diagrams, are of vibrational nature.
From a qualitative point of view, the comparison with the pressure trend is good; in the future a quantitative analysis will be performed in order to assess a complete monitoring of the I.C. engine system through the vibrational morphodynamics. Furthermore, the analysis of the behavior by means of this methodology can be used for analyzing how the engine changes its morphodynamics signature and for verifying how the combustion occurs. It defines a functional map of the engine vibration for each sequence of parameters such as crank angle, EGR ratio and the characteristics of combustion.

The results carried out show that little variations well define the repeatability classes of the EGR demonstrating that the morphodynamics analysis “feels” the system changing and can verify the instability conditions before they occur. Finally an application to a mechanical system represented by a mechanical hand prosthesis was also presented. Further investigations in all the presented fields were planned.

REFERENCES

[1] Gille B.A., *History of technology and invention, progress through the ages*. Maurice Daumas, New York, Vol. I, 1969.

[2] Daubechies I., Orthonormal bases of compactly supported wavelets. *Communications in Pure and Applied Mathematics*, 1988.

[3] Meyer Y., *Wavelets: algorithms and applications*. SIAM: Philadelphia, 1993.

[4] Wickerhauser M.V., *Adapted wavelet analysis from theory to software*. IEEE Press, AK Peters, Natick, Massachusetts, 1994.

[5] Jinyoung C., Junhong K., Youngjin C., Simsoo P., The effect of exhaust gas recirculation (EGR) on combustion stability, engine performance and exhaust emissions in a gasoline engine. *KSME Journal*, Vol. 15, No. 10, pp 1442-1450, 2001.

[6] Haiyong P., Yi C., Lei S., Kangyao D., Effects of EGR on combustion process of DI diesel engine during cold start. *Front. Energy Power Eng. China*, Vol. 2, No. 2, pp. 202-210, 2008.

[7] Molin J., Investigation of correlations between COV of ion integral and COV of IMEP in a port-injected natural-gas engine. *Master thesis*, Linköping, 12 December, 2008.

[8] Wasiu S.O., Sulaiman S.A., Aziz A.R.A., An experimental study of different effects of EGR rates on the performance and exhaust emissions of the stratified charge piston direct injection compressed natural gas engine. *Journal of Applied Sciences*, Vol. 11, No. 9, pp. 1479-1490, 2011.

[9] Li H., Karim G.A., Modeling the performance of turbo-charged spark ignition natural gas engine with cooled exhaust gas recirculation. *Journal of Engineering for Gas Turbine and Power*, Vol. 130, May 2008.

[10] Amoresano A., Niola V., Quaremba A., A sensitive methodology for the EGR optimization: a perspective study. *Int. Review of Mechanical Engineering (I.RE.M.E.)*, Vol. 6, No. 5, 2012. ISSN 1970 - 8734.

[11] Amoresano A., Avagliano V., Niola V., Quaremba G., The assessment of the in-cylinder pressure by means of the morpho-dynamical vibration analysis - Methodology and application. *Int. Review of Mechanical Engineering,* Vol. 7, No. 6, 2013. ISSN 1970-8734.

[12] Niola V., Quaremba G., Amoresano A., A study on infrared thermography processed trough the wavelet transform. *Proc. of 8th WSEAS International Conference on System Science and Simulation in Engineering, ICOSSSE '09*, pp. 57-62, 2009.

[13] Rossi C., Savino S., Mechanical model of a single tendon finger. *Proc. of 11th International Conference of Numerical Analysis and Applied Mathematics*, Rhodes; Greece, 21 September, Vol. 1558, pp. 1286-1292, 2013.

[14] Rossi C., Savino S., Niola V., Troncone S., A study of a robotic hand with tendon driven fingers. *Robotica*, Vol. 33, No. 5, doi: 10.1017/S0263574714001179, ISSN: 0263-5747, pp. 1034-1048, 2014.

[15] Niola V., Rossi C., Savino S., A new mechanical hand: Theoretical studies and first prototyping. *Int. Review of Mechanical Engineering*, Vol. 8, No. 5, ISSN:19708734, pp. 835-844, 2014.

[16] Rossi C., Savino S., Robot Trajectory planning by assigning positions and tangential velocities. *Robotics and Computer Integrated Manufacturing*. Vol. 29, No. 1, doi: 10.1016/j.rcim.2012.04.003, pp. 139-156, 2013.

[17] Niola V., Rossi C., Savino S., Strano S., Robot trajectory planning by points and tangents. *Proc. of 10th WSEAS Int. Conference on Robotics, Control and Manufacturing Technology*, Hangzhou, China, April 11-13, ISSN: 1790-5117 91, ISBN: 978-960-474-175-5, pp. 91-96, 2010.